



Sensors for ultra-fast silicon detectors



H.F.-W. Sadrozinski^{a,*}, M. Baselga^{a,1}, S. Ely^{a,2}, V. Fadeyev^a, Z. Galloway^a, J. Ngo^a, C. Parker^a, D. Schumacher^a, A. Seiden^a, A. Zatserklyaniy^a, N. Cartiglia^b, G. Pellegrini^c, P. Fernández-Martínez^c, V. Greco^c, S. Hidalgo^c, D. Quirion^c

^a Santa Cruz Institute for Particle Physics, UC Santa Cruz, Santa Cruz, CA 95064, USA

^b INFN Torino, Torino, Italy

^c Centro Nacional de Microelectrónica, IMB-CNM-CSIC, Barcelona, Spain

ARTICLE INFO

Available online 14 May 2014

Keywords:

Fast silicon sensors
Charge multiplication
Thin tracking sensors
Silicon strip
Pixel detectors

ABSTRACT

We report on electrical and charge collection tests of silicon sensors with internal gain as part of our development of ultra-fast silicon detectors. Using $C-V$ and α TCT measurements, we investigate the non-uniform doping profile of so-called low-gain avalanche detectors (LGAD). These are n-on-p pad sensors with charge multiplication due to the presence of a thin, low-resistivity diffusion layer below the junction, obtained with a highly doped implant. We compare the bias dependence of the pulse shapes of traditional sensors and of LGAD sensors with different dopant density of the diffusion layer, and extract the internal gain.

© 2014 Elsevier B.V. All rights reserved.

1. Introduction

We propose an ultra-fast silicon detector (UFSD) that will establish a new paradigm for space-time particle tracking [1]. Presently, precise tracking devices determine time quite poorly while good timing devices are too large for accurate position measurement. This fact is imposing severe limitations on the potential of many applications ranging from medical positron emission tomography (PET) to mass spectroscopy or particle tracking.

We plan to develop a single device able to concurrently measure with high precision the space ($\sim 10 \mu\text{m}$) and time ($\sim 10 \text{ps}$) coordinates of a particle. Our analysis of the properties of silicon pixel detectors, which already have sufficient position resolution, indicates that it is possible to improve their timing characteristics to achieve this goal. In order to obtain the high signal-to-noise ratio (S/N) needed for UFSD, we will use and control the silicon sensors internal charge multiplication mechanism. This is a recent, very active field of investigations within the CERN based RD50 collaboration [2].

The development of UFSD research is poised to open up a range of new opportunities for applications that benefit from the combination of position and timing information. As explained in more detail in Ref. [3], UFSD will help sharpen PET images and

monitor more accurately the dose delivered in cancer treatment. UFSD will increase the precision of time of flight (ToF) measurement in applications like mass spectroscopy, robotic vision and particle identification. Additionally, UFSD can improve particle tracking by suppressing random accidental coincidences in high-rate experiments as planned in High-Energy Physics.

UFSD are pixelated silicon sensors based on the LGAD design. In the following, we describe the principle, properties and expected performance of the UFSD. Then, we discuss the observation of internal gain in silicon sensors, a crucial part of UFSD, and the description of LGAD. We present data on $I-V$ and $C-V$ measurements, correlated with results from α TCT measurements, which provide both pulse shape and charge collection information and allow determination of the gain.

2. Principle of UFSD

High-rate operation of silicon sensors faces the obstacle that the drift velocity in silicon saturates at about 10^7cm/s , and thus the collection time of electrons inside a silicon layer of $300 \mu\text{m}$ thickness is limited to $\sim 3 \text{ns}$. Fast silicon sensors need therefore to be very thin and be able to function even though the charge collected is reduced with respect to that of thicker sensors. However, since the time resolution of a sensor depends on the signal-to-noise ratio S/N , the charge collected from a thin active layer might not be enough to achieve good time resolution. To overcome this limitation, we propose to exploit charge multiplication to increase the

* Corresponding author. Tel.: +1 831 459 4670; fax: +1 831 459 5777.

E-mail address: hartmut@scipp.ucsc.edu (H.F.-W. Sadrozinski).

¹ Permanent address: Centro Nacional de Microelectronica, CNM-IMB (CSIC), Barcelona, Spain.

² Present address: Dept. of Physics, Syracuse Univ., Syracuse, NY 13210, USA.

charge yield of very thin silicon sensors so that they can be used in ultra-fast timing applications [1,3].

2.1. Internal gain in silicon sensors

It has been demonstrated that in silicon sensors the charge multiplication factor, which is responsible for the charge gain (similar to the first Townsend coefficient [4] in gas multiplication), has an exponential dependence on the electric field [5,6]. Close to breakdown, at an electric field of $E=300$ kV/cm, the achievable multiplication reaches $\sim 0.66/\mu\text{m}$ for electrons and $\sim 0.17/\mu\text{m}$ for holes.

As shown by simulation [7], planar sensors with uniform low doping density cannot obtain such an extended high-field region needed for avalanche charge multiplication. Moderate internal gain has been observed in silicon sensors after irradiation by several groups due to the non-uniformity of the electric field [8–11]. Thus, in order to have silicon sensors with internal gain, a non-uniform doping profile similar to silicon photomultipliers (SiPM) [12,13] or multi-pixel photon counters (MPPC) [14] is required, as explained in the next section.

2.2. Low-gain avalanche detectors (LGAD)

Low-gain avalanche detectors (LGAD), as developed by Centro Nacional de Microelectronica (CNM) [15,16], are n-on-p silicon sensors with a 300 μm thick high-ohmic Float Zone (FZ) p-bulk which have a p+ implant extending a few microns underneath the n-implant. This implant generates a large local field at a depth of about 1–5 μm , as shown in Fig. 1 [7]. The doping concentration of the p+ implant is chosen to generate a gain of 10–100, in contrast to a gain of 10^4 or more in SiPM and MPPC. LGAD sensors work by inducing multiplication for electrons, while the multiplication of holes, given the field and depth values involved, is less important. Therefore, LGAD sensors do not have a large positive feedback loop formed by concurrent electron and hole multiplication processes, present in SiPM, which causes the avalanche and the subsequent dead time. At sufficiently high bias voltage, the drift field in the remainder of the 300 μm deep bulk can be almost as high with the p+ implant (“Gain”) as in sensors without it (“No Gain”), and thus the large drift field > 20 kV/cm needed for fast collection of the charges [17] can be established.

2.3. Gain requirements for ultra-fast timing

Charge multiplication in silicon sensors allows increasing the signal-to-noise ratio S/N as long as the extra noise due to the

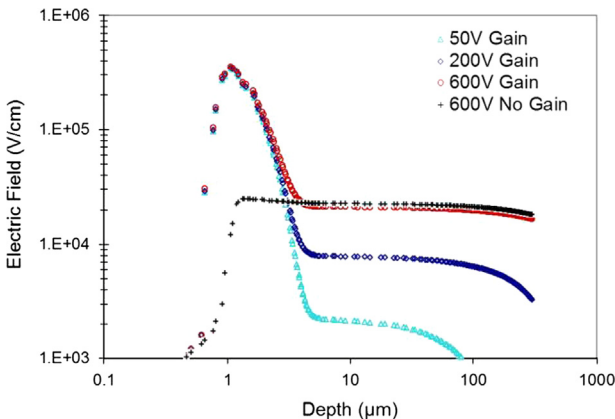


Fig. 1. Simulation of electric field profile in a LGAD (“Gain”) for several bias voltages compared to the field in a pad sensor without gain (“No Gain”) [7].

multiplication process is small, which is true for fast sensors with shaping time below 1 ns, gain of about 10, and leakage current of the order 1 nA per pixel or less [18].

The time resolution σ_t , ignoring small effects due to TDC binning, can be parameterized as:

$$\sigma_t = \left[\left(\frac{N}{S} \right)^2 + \left(\frac{\Delta S S_{thr}}{S} \right)^2 \right]^{1/2},$$

where S is the pulse amplitude, τ_R its rise time, N the jitter due to the electronic noise and $\Delta S/S$ the time walk due to the amplitude dispersion from the Landau distribution [19] with respect to a fixed threshold S_{thr} . In the following, the rise time will be set equal to the collection time to get optimal timing performance, and this correlates the rise time and the sensor thickness. Following Ref. [20], we will assume (i) a noise $N=1000e^-$ at a shaping time of 500 ps, and (ii) the noise scaling like $1/\sqrt{\tau_R}$ with the shaping time. These assumptions are consistent with the measured noise on the ATLAS pixels [21]. Furthermore, when assuming (iii) the threshold be set at $10 \times N$ to suppress noise counts, and (iv) a reduction of the time walk by a factor CFD due to the use of a constant fraction discriminator [20], the time resolution can be expressed as:

$$\sigma_t(\text{CFD}) = \tau_R \frac{1}{(S/N)} \left[1 + \left(\text{CFD} \times 10 \frac{\Delta S}{S} \right)^2 \right]^{1/2}.$$

For high-rate sensors, we look for the fastest rise time with a realistic $S/N > 30$. Then the time resolution depends on the gain as shown in Table 1, with a marked improvement with the use of a constant fraction discriminator even with a modest $\text{CFD}=1/3$. For a gain $G=10$, a rise time of $\tau_R=800$ ps and a sensor thickness of 36 μm the time resolution will be 30–40 ps.

3. Electrical properties of low-gain avalanche detectors (LGADs)

The electrical properties of LGADs are probed with current–bias voltage (I – V) and capacitance–bias voltage (C – V) measurements. Under the assumption of a uniform planar diode, the C – V data are used to extract the depth of the depleted region x and an estimate of the doping profile.

3.1. Comparison with no-gain diodes

Fig. 2 shows a comparison of C – V curves between a LGAD and a pad sensor without gain. The bias dependences of $1/C^2$ (Fig. 2a) and of the depth of the depleted region (Fig. 2b) shows for the LGAD a shift in the depletion of the bulk due to the need to deplete the p+ implant located directly below the junction. The apparent step in the capacitance curve at bias of ~ 100 V for the LGAD and ~ 50 V for the no-gain pad (corresponding to an apparent depth of the about 200 μm in both sensors) is still being investigated but it is believed to be caused by a fairly complex interplay between the oxide charge on the surface and the deep implant at the edge of the n+ electrode in the process of lateral depletion [7].

Table 1
Time resolution for fastest rise time allowed by $S/N > 30$ as a function of gain.

Gain G	τ_R [ps]	Thickness [μm]	Time resolution [ps]			
			No CFD	CFD=1/10	CFD=1/5	CFD=1/3
1	3000	130	282	132	139	154
10	800	36	85	30	33	40
100	200	9	29	7.5	9.0	11.6

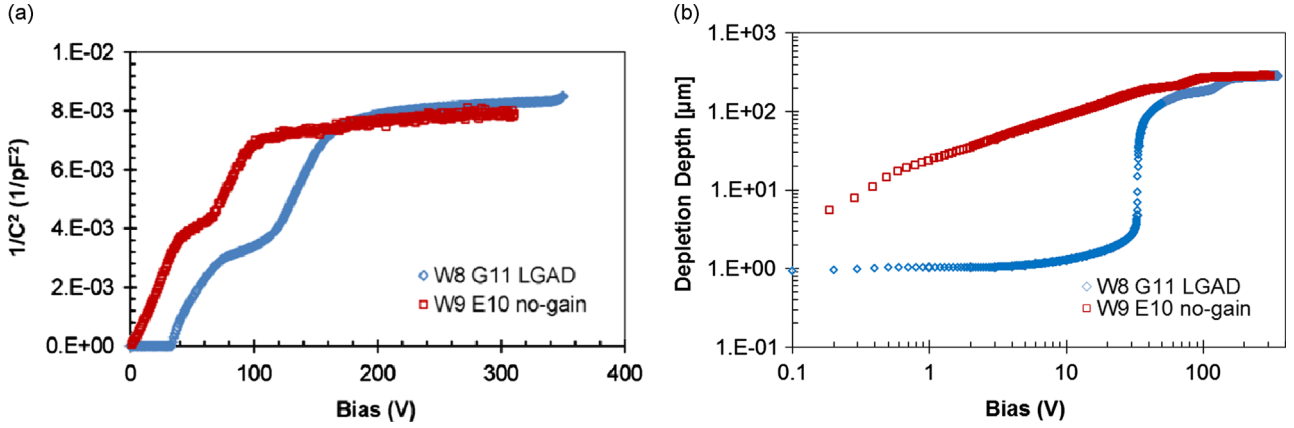


Fig. 2. Electric parameters of two pad sensors with (LGAD) and without gain: (a) $1/C^2$ vs. bias voltage and (b) the depth of the depleted region.

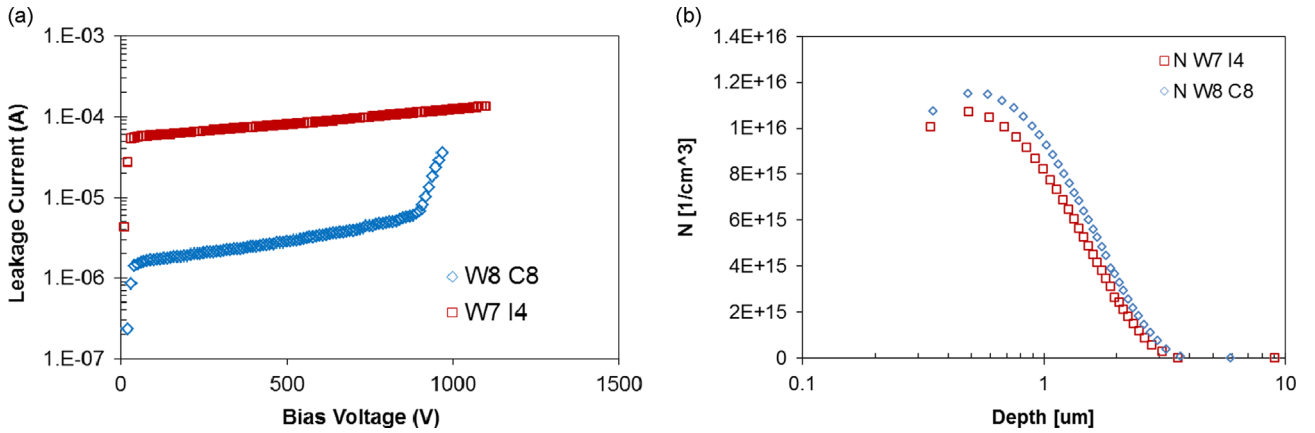


Fig. 3. Electric parameters of two LGAD pad sensor with gain: (a) I - V curves (b) doping density, N , within the p^+ implant depth vs. depth extracted from the C - V data.

3.2. Comparison of LGAD with different leakage currents

It has been argued that the leakage current in LGAD should be subject to the same multiplication factor as the particle signals [22]. We have investigated two LGAD with leakage currents differing by a factor of about 100 (Fig. 3a) to verify that. We observe good breakdown behavior up to 900 V. We extract the doping density from the C - V measurements using the fact that the slope of the $1/C^2$ vs. V curve is related to it. The data indicate a doping density about 10% higher in the low leakage current device W8-C8 with respect to the high current device W7-I4 (Fig. 3b). The p^+ doping excess of W8-C8 over W7-I4 inferred from the manufacturing data was 20% [23]. For the no-gain diode W9-E10 the doping density is measured to be constant at $2 \times 10^{12} \text{ cm}^{-3}$ up to $2 \mu\text{m}$ from the junction, the smallest depth we could measure.

From these observations we can conclude that the diode with higher dopant concentration has significantly smaller leakage current, indicating no correlation between these parameters. On the contrary, there is expected correlation of the doping density with gain, as it is shown in Section 4.

4. TCT in un-irradiated LGAD and no-gain sensors

We expect the pulse shapes in charge collection studies to reveal details of the charge collection dynamics in the sensors. Both LGAD and no-gain pad sensors with the same geometrical details are used in a time-resolved charge transient (TCT) study

with α particles from an Am(241) source. The sensors are read out with a MiteQ amplifier AM-1607-3000, which has a gain of 40 dB and a band pass of 10 kHz to 3 GHz. The output of the amplifier is connected to a Tektronics oscilloscope DPO 7254 with 2.5 GHz bandwidth. The α particles enter in the low-field region on the backside of the sensor (on the right in Fig. 1), where they are absorbed within a few microns. Current vs. time waveforms are recorded during the drift through the entire bulk and the high-field region to the front of the sensor (on the left in Fig. 1). In TCT language this is called electron injection.

4.1. Pulse shapes in α TCT

Fig. 4 shows pulse shapes at two different bias voltages for the two LGAD discussed in Section 3.2 and a no-gain diode. At a bias above 900 V, the pulse durations of all 3 sensors reach their minima due to saturation of drift velocity. All pulses are characterized by a leading part of about 3 ns duration which can be identified with the drift of the primary electrons. In the following, it is called the “initial pulse”. For the LGAD, the initial pulses are followed by a longer signal from the electrons and holes generated in the charge multiplication, with the holes taking about 2 ns longer than the initial pulse duration to drift back to the back plane. This signal from the multiplication process is absent in the TCT signal of the no-gain diode, and varies in strength between the two LGADs selected. The collected charge is calculated separately for the initial pulse and for the total pulse by integrating them and dividing them by the input resistance of the amplifier (50 Ω).

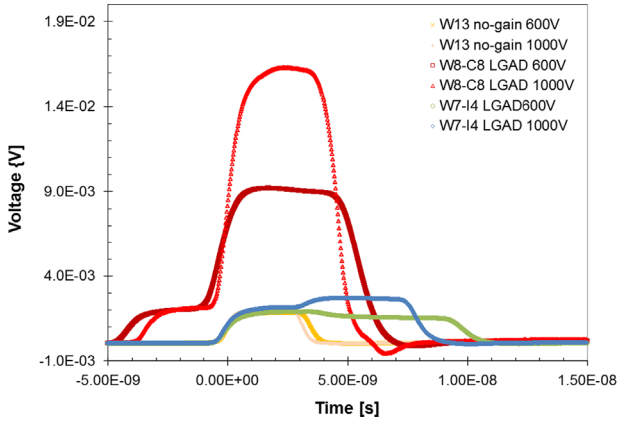


Fig. 4. α TCT pulse shapes from electron injection for two LGAD and a no-gain diode at two bias voltages.

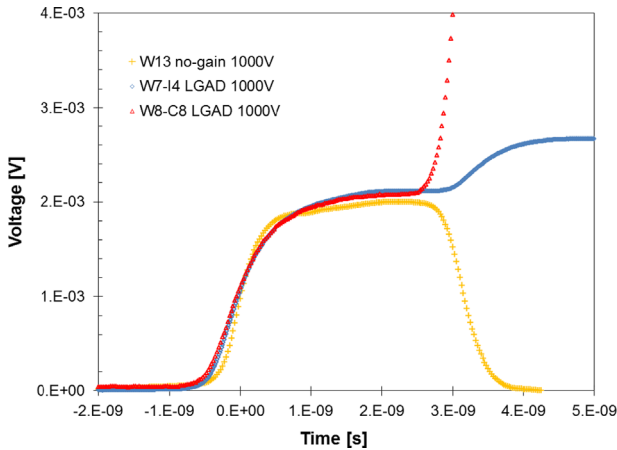


Fig. 5. Initial α TCT pulse shapes from electron injection for two LGAD and a no-gain diode at 1000 V bias.

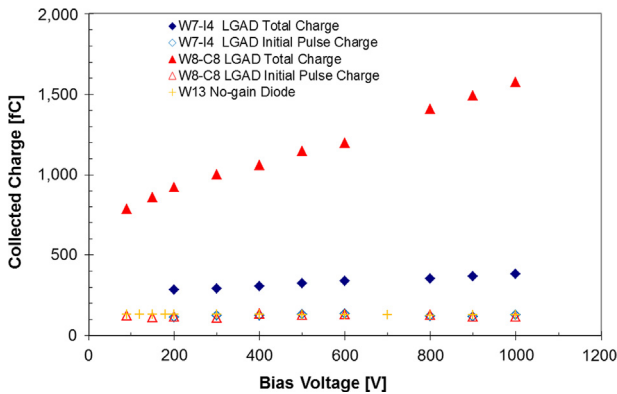


Fig. 6. Bias dependence of initial pulse charge and the total charge for two LGAD with a 20% different $p+$ implant dose and the total charge of a no-gain diode.

4.2. The initial α TCT pulse

The initial pulses of the LGAD are compared in Fig. 5 with the total pulse of the no-gain diode. For the first three ns, the three pulses match very well, proving their common origin. The charge in the initial pulse of the LGAD can be determined only up to the “cut-off” time when the pulse due to the multiplication process starts. This deficit in the charge of the initial pulse of the LGAD can be corrected by estimating the fraction of charge in the pulse of the no-gain diode beyond the cut-off time. The correction factor amounts to 1.13 for W8-C8 and 1.06 for W7-I4, respectively. The

collected charges for the initial pulses of the LGADs and the total pulse of the no-gain diode are shown in Fig. 6 as a function of bias voltage. The bias voltage dependence is less than 1%, and the averages of the three agree within 5%. These results validate our identification of the initial pulse with the initial electron drift, for which the collected charge should be independent of the bias voltage. They also indicate that the systematics of our α TCT set-up are under control.

The collected charge of the no-gain diode corresponds to an absorbed energy of 2.92 MeV, about 54% of the α energy from the Am(241) decay. The energy difference can be explained by energy losses in the Pd window of the source, in the air and in a thin inert Si layer in the detector.

4.3. Gain derived from α TCT pulse shapes

The collected charge of both initial pulse and the total pulse are shown in Fig. 6 as a function of the bias voltage. The total charge for the LGADs increases monotonically with bias, while the initial pulse charge is constant, as mentioned before. Defining the gain as the ratio $G = (\text{total charge}) / (\text{corrected initial charge})$, we observe an almost linear increase in gain when increasing the bias from 200 V to 1000 V: from $G = 8.0$ to $G = 13.6$ for W8-C8 and $G = 2.5$ to $G = 3.0$ for W7-I4. Even at a low bias voltage of 90 V, we observe a gain $G = 6$ for W8-C8. There is clearly a difference in gain between the two LGAD shown: $G(\text{W8-C8}) / G(\text{W7-I4}) \approx 4$ at 1000 V bias. Given that W8-C8 has much lower current than W7-I4, as mentioned in Section 3.2, the data do not support the notion that the leakage current scales with the gain.

On the other hand, as mentioned before, W8-C8 has a higher $p+$ implant dose than W7-I4. Taking the increase in $p+$ dose to be 20% as in the fabrication specifications, this corresponds to a gain increase of $\Delta G / G = 0.15$ for 1% increase in $p+$ dose, showing the extreme sensitivity of the gain on the $p+$ dose, which also has been reported in Ref. [23].

5. Conclusions

We are pursuing the development of ultra-fast silicon detectors UFSD, which are estimated to be able to reach 10 ps timing resolution in addition to the fine spatial resolution typical for silicon sensors. A crucial part of UFSD is the use of sensors with internal gain.

We investigate the correlation between required shaping time, sensor thickness and the expected time resolution for sensors as a function of the gain.

Low-gain avalanche detectors (LGAD) have been identified as suitable candidates for UFSD. In electrical testing of the LGAD, we find high breakdown voltages in I - V curves and strong non-linear effects in C - V measurements due to the non-uniformity of the doping profile.

We analyze pulses in α TCT study in terms of the charge collection during the initial electron drift and the subsequent collection of electron and holes generated in the charge multiplication process. This allows the normalization of the gain, which is rising almost linearly with the bias.

We find a strong dependence of the gain on the dose of the low-resistance p -implant, which is responsible for the gain process. Differences up to a factor of 4 were measured for diodes with doping density difference of 20%.

We do not find the level of leakage current to be correlated with the gain values for the sensors we measured.

The highest gain measured in our samples was about 14 at 1000 V bias for the LGAD sensor with low leakage current and high $p+$ implant dose.

Acknowledgments

We thank Gregor Kramberger for sharing his data, our RD50 colleagues for fruitful discussions on sensors, and Angelo Rivetti for helping us understand the readout issues. We acknowledge the expert technical help of Max Wilder and Forest Martinez-McKinney.

Part of this work has been performed in the framework of the CERN RD-50 collaboration and (partially) financed by the Spanish Ministry of Education and Science through the Particle Physics National Program (FPA2010-22060-C02-02 and FPA2010-22163_C02-02). Marta Baselga acknowledges a stipend from the Spanish Ministry of Science and Innovation (FPA2010-22060-C02-02). The work at SCIPP was partially supported by the United States Department of Energy, grant DE-FG02-04ER41286.

References

- [1] H.F.-W. Sadrozinski, Exploring charge multiplication for fast timing with silicon sensors, in: Twentieth RD50 Workshop, Bari, Italy, May 30–June 1, 2012, and References therein (<https://indico.cern.ch/conferenceOtherViews.py?view=standard&confid=175330>).
- [2] RD50 Collaboration, (<http://rd50.web.cern.ch/rd50/>).
- [3] H. F.-W. Sadrozinski, et al., Ultra-Fast Silicon Detectors, RESMDD12, Nuclear Instruments and Methods in Physics Research Section A, in print.
- [4] J.S. Townsend, *Electricity in Gases*, Oxford at the Clarendon Press, 1915.
- [5] A. Macchiolo, Impact ionization in silicon detectors, in: Sixteenth RD50 Workshop Barcelona, Spain, 2010, (<http://indico.cern.ch/getFile.py/access?contribId=1&sessionId=3&resId=0&materialId=slides&confId=86625>).
- [6] W. Maes, K. De Meyer, R. Van Overstraeten, Impact ionization in silicon, a review and update, *Solid-State Electronics* 33 (6) (1990) 705.
- [7] C. Parker, Realization of Planar Silicon Sensors for Fast Timing Experiments. UC Santa Cruz Physics, Master of Science Thesis, September 2013. As of 27 April 2013, it is available at (<http://adap.ucsc.edu/theses/ColinParkerMaster.pdf>).
- [8] I. Mandic, et al., Study of anomalous charge collection efficiency in heavily irradiated silicon strip detectors, *Nuclear Instruments and Methods in Physics Research Section A* 636 (Suppl.) (2011) S50.
- [9] G. Casse, et al., Enhanced efficiency of segmented silicon detectors of different thicknesses after proton irradiations up to 1×10^{16} neq cm^2 , *Nuclear Instruments and Methods in Physics Research Section A* 624 (2) (2010) 401.
- [10] M. Kohler, et al., Comparative studies of irradiated 3D silicon strip detectors on p-type and n-type substrate, in: Seventh RD50 Workshop CERN Switzerland, 17–19 November 2010, (<http://indico.cern.ch/getFile.py/access?contribId=4&sessionId=4&resId=0&materialId=slides&confId=111191>).
- [11] J. Lange, et al., Properties of a radiation-induced charge multiplication region in epitaxial silicon diodes, *Nuclear Instruments and Methods in Physics Research Section A* 622 (2010) 49.
- [12] C. Piemonte, A new silicon photomultiplier structure for blue light detection, *Nuclear Instruments and Methods in Physics Research Section A* 568 (2006) 224.
- [13] G.-F. Dalla Betta, et al., High-performance PIN photodiodes on TMAH thinned silicon wafers, *Microelectronics Journal* 39 (2008) 1485.
- [14] T. Nagano et al., Timing Resolution Improvement of MPPC for TOF-PET Imaging, 2012 IEEE NSS-MIC, Anaheim, CA, Oct 29–Nov 3, 2012.
- [15] P. Fernandez, et al., Simulation of new p-type strip detectors with trench to enhance the charge multiplication effect in the n-type electrodes, *Nuclear Instruments and Methods in Physics Research Section A* 658 (2011) 98.
- [16] G. Pellegrini et al., Measurements of low gain avalanche detectors (LGAD) for high energy physics applications, in: This Conference.
- [17] G. Kramberger, et al., Electric field and space charge in neutron irradiated n+–p sensors, in: Nineteenth RD50 Workshop CERN, Switzerland, Nov. 21–23, 2011, (<http://indico.cern.ch/getFile.py/access?contribId=7&sessionId=1&resId=0&materialId=slides&confId=148833>).
- [18] R.J. McIntyre, *IEEE TED13*(1966) 164.
- [19] S. Meroli, D. Passeri, L. Servoli, *JINST* 11 (2011) (6 P06013).
- [20] A. Rivetti, Private Communication.
- [21] D. Dobos, Overview of the ATLAS IBL project, in: This Conference.
- [22] G. Kramberger, et al., Studies of CNM diodes with gain, in: Twentieth RD50 Workshop, Albuquerque, NM, USA, June 3–5, 2013, (<https://indico.cern.ch/getFile.py/access?contribId=28&sessionId=3&resId=0&materialId=slides&confId=209612>).
- [23] S. Hidalgo, et al., Simulation and technology developments of low gain avalanche detectors (LGAD) for high energy physics applications, in: Twentieth RD50 Workshop, Albuquerque, NM, USA, June 3–5, 2013, (<https://indico.cern.ch/getFile.py/access?contribId=4&sessionId=3&resId=0&materialId=slides&confId=209612>).